 doi:10.20944/preprints202011.0573.v1

Electronic, magnetic and optical properties of $XScO_3$ (X=Mo, W) perovskites

Amall A. Ramanathan* and J.M. Khalifeh

*Corresponding author Email:a.ramanathan@ju.edu.jo

The University of Jordan, Department of Physics, Amman-11942, Jordan

Abstract

Density Functional Theory (DFT) full potential linearized augmented plane wave (FP-LAPW) method with the Modified Becke-Johnson (mBJ) approximation is used to perform spin polarised calculations of the transition metal perovskites $MoScO_3$ and $WScO_3$. Both depict half metallic behaviour with semiconducting and metallic in the minority and majority spins respectively. $MoScO_3$ and $WScO_3$ have indirect R− Γ band gaps in the minority spin channels of 3.61 and 3.82eV respectively. Moreover, they both show substantial magnetic moments of $2.99\mu_B$. In addition, we calculate the dielectric function, optical conductivity and the optical constants, namely, the refractive index, the reflectivity, the extinction and absorption coefficients.

Key words: DFT-mBJ; magnetic moments, optical conductivity, perovskites

 doi:10.20944/preprints202011.0573.v1

1. Introduction

The recent years has seen a lot of research on perovskites for potential applications in electronics, photovoltaics, renewable energy and innumerable other industries [1-3]. The universal structural formula of a perovskite is ABX_3 and the cubic form is the most ideal case. X atom is usually oxygen. It could also be a halide. A/B atoms are in general alkali, alkali earth, rare earth or transition metals [4, 5]. Thus, an enormous variety of structural modifications and variants are possible which can accommodate almost all of the elements in the periodic Table. The flexibility in choice of atom types gives rise to a multitude of perovskite structures with interesting electronic, magnetic and optical properties and motivates the continued interest in this family [6-8].

Transition metals (TM) are exceptionally valuable and allow for complex magnetic interactions depending upon the local environment and dimensionality to give intriguing magnetic, magneto-electric, multiferroic, piezoelectric properties [9-11] and even induce non-magnetic materials to become magnetic [12, 13]. Thus, transition metal (TM) perovskites are of special interest and past research show a wide range of electronic, magnetic and optical properties owing to the complex nature of TM ion interactions with oxygen or halides [14, 15]. It is mainly the unfilled or filled'd' bands of the TM that are responsible for the electronic/magnetic and dielectric properties respectively.

In most of the previous studies on TM perovskites, the TM occupies the B site. Recently, we explored the effect of 3d-filling on the electronic, magnetic and optical properties on $TMScO_3$ perovskites where the TM (from Ti to Zn) sits on the A site [16]. The materials show half metallic behavior with wide band gaps, except for $TiScO_3$ and $VScO_3$ which are metallic and semiconducting. As, a further study, in the current work we explore the electronic, magnetic and optical properties with TM Mo and W which are isoelectric to Cr in group VI i.e. $MoScO_3$ and $WScO_3$ perovskites. The purpose of the paper is to give the essential and accurate theoretical information of the optoelectronic properties of these perovskite compounds, which are being investigated for the first time for possible technological applications and further research.

The perovskites $MoScO_3$ and $WScO_3$ are investigated using the full-potential linearized augmented plane wave (FP-LAPW) DFT method with the wein2k software program. The paper is arranged as follows: section 2 gives the Calculation details, section 3 is devoted to the Discussion of results under the sub headings_ Structural and electronic; Magnetic and Optical properties, finally section 4 presents the Conclusions.

2. Calculation details

The full-potential linearized-augmented plane wave (FP-LAPW) method as implemented in the WIEN2k [17] code based on DFT [18] is used to calculate the spin polarized ground states of the pervoskites. We have used generalized gradient approximation (GGA) of Perdew, Burke and Ernzerhof (PBE) [19] to calculate the optimized structures at a 10×10×10 kpoint grid. The optimized lattice constant values have then been used with the more accurate Modified Becke-

Preprints (www.preprints.org) | NOT PEER-REVIEWED | Posted: 23 November 2020 doi:10.20944/preprints202011.0573.v1

Johnson (mBJ) exchange correlation of Trans Blaha [20] to evaluate the electronic, magnetic and optical properties using denser grids of 15×15×15 and 30×30×30 for electronic/magnetic and optical properties respectively.

In order to achieve energy eigenvalues convergence, the wave functions in interstitial region were expanded in plane waves with a cutoff of Kmax set to 8; Kmax gives the magnitude of the largest K vector in the plane-wave expansion. The muffin-tin radii (RMT), which denotes the smallest atomic sphere radius are taken to be 2.5 and 2.7 a.u for Mo, W respectively and 1.60 a.u for Sc and O atoms. The Brillouin zone integrations within the self-consistency cycle are performed via a tetrahedron method [21] using 120 k points in the irreducible wedge of the Brillouin zone (IBZ) for all compounds. The self-consistence calculations have convergence tolerance thresholds of less than 10^{-4} Ry in energy and 10^{-4} in electron charges.

3. Discussion of Results

3.1 Structural and electronic properties

The $MoScO_3$ and $WScO_3$ Perovskites in the cubic form with space group is Pm-3m (#221) contains one formula unit and the Mo/W, Sc and O atoms are positioned at 1a (0, 0,0), 1b (½, ½,½) and 3c (0,½, ½) sites of Wyckoff coordinates, respectively.

The lattice constants of $XScO_3$ structures are optimized using Murnaghan equation of state [22] and the energy vs volume curves are presented in Figure1 along with the structure visualization. Since, the structure is cubic only volume optimization is required.

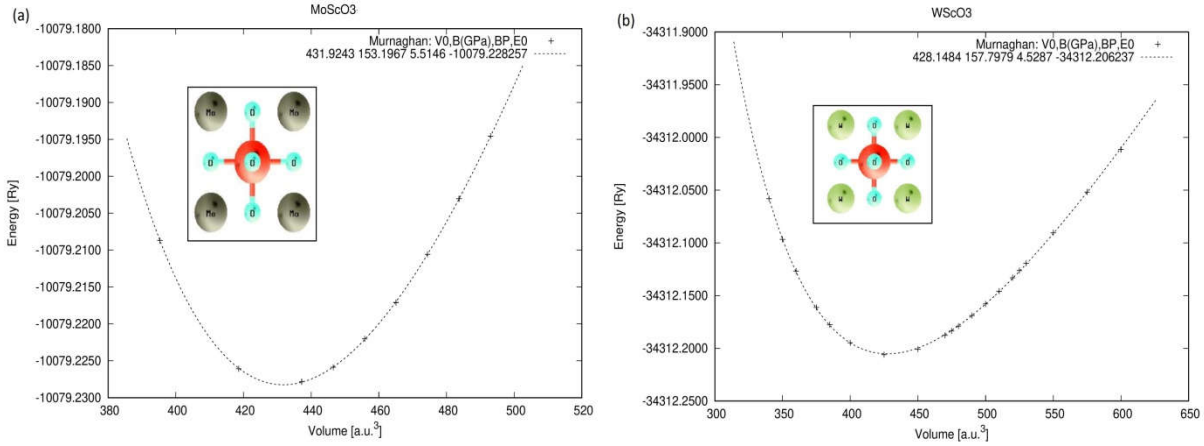

Fig. 1 The volume optimization Murnaghan fit curves for (a) $MoScO_3$ and (b) $WScO_3$

The optimized lattice constants, bulk moduli, Fermi and total energies at the minimum energy equilibrium state are shown in Table 1.

We notice that the lattice constant of the perovskites decreases slightly with increasing atomic numbers of the TM. Although, the individual ionic radii of Mo and W are comparable the decrease in size of the compounds can be attributed to the change in electronic density and changes in the occupation of the band orbitals in new molecular environment.

Preprints (www.preprints.org) | NOT PEER-REVIEWED | Posted: 23 November 2020 doi:10.20944/preprints202011.0573.v1

Table 1 Optimized Structural parameters

Perovskites	Lattice constant a [Å]	Bo [GPa]	Total Energies[Ry]
$MoScO_3$	4.000	153.197	-10079.2282
$WScO_3$	3.988	157.798	-34312.2068

The mbj exchange potential has consistently proved to give accurate and very reliable band structures comparable to that of GW or hybrid functionals. After the structural optimization using GGA-PBE, our electronic and optical calculations have been performed using mBJ to obtain highly accurate band structures of the perovskites and reliable results for all the optical properties under investigation. The $MoScO_3$ and $WScO_3$ band structures along the high symmetry points are shown in Figures 2 and 3 respectively.

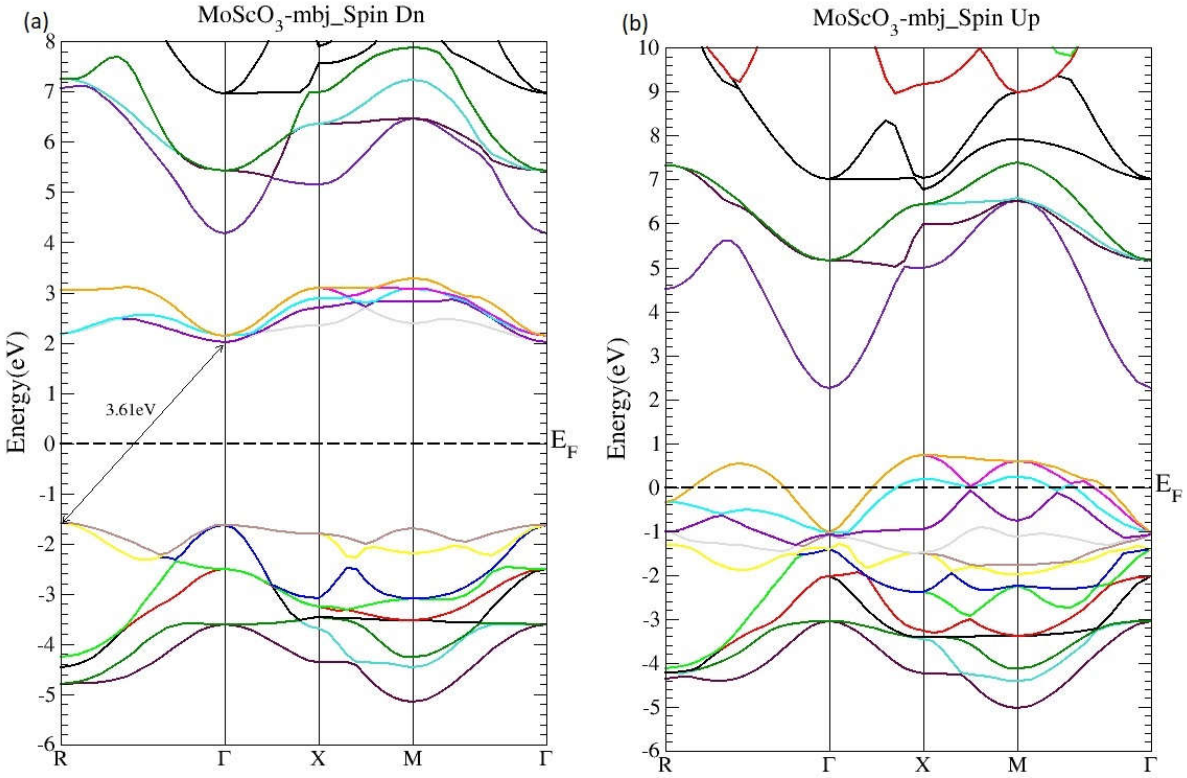

Fig. 2 The $MoScO_3$ electronic band structures for (a) the minority (Spin Dn) and (b) the majority (Spin Up) channels

As seen from Fig. 2, $MoScO_3$ shows interesting semi-conducting behavior in the minority spin with an indirect R−Γ of 3.61eV which predominates over the direct Γ−Γ gap of 3.64eV. In fact we see that the difference between valence band maximum (VBM) at the R and Γ points are very close, with just a difference of 0.033eV. A direct bandgap is very favorable since excitation is

Preprints (www.preprints.org) | NOT PEER-REVIEWED | Posted: 23 November 2020 doi:10.20944/preprints202011.0573.v1

possible with photons of energy equivalent or higher than the band gap, and gives stronger emission or absorption properties for potential applications in photovoltaics (PV), light emitting diodes (LED) etc. The indirect band gap requires both a photon and phonon for excitation of electrons from the valence to conduction band; nevertheless, it has also useful applications in optoelectronics. The Majority channel in Fig.2 (b) shows a slight metallic behavior with only very few valence bands at the beginning of the conduction band.

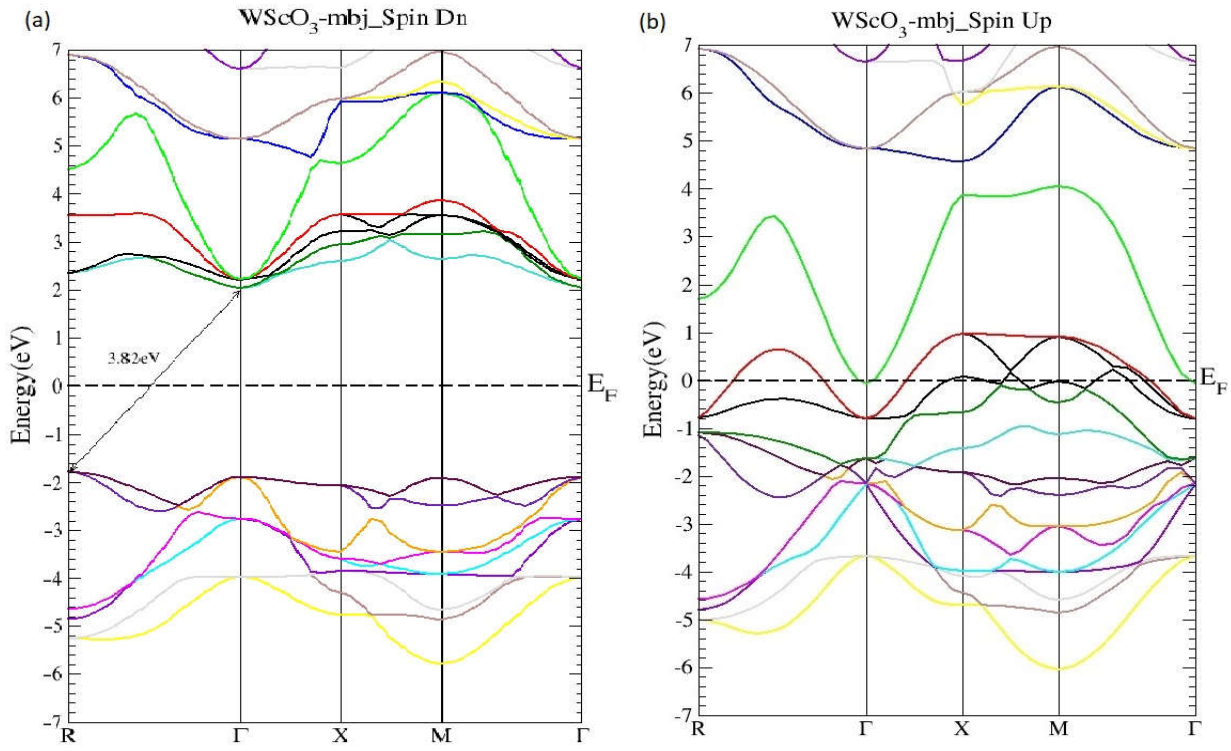

Fig. 3 The $WScO_3$ electronic band structures for (a) the minority(Spin Dn) and (b) the majority(Spin Up) channels

In Fig. 3 the $WScO_3$ band structures are depicted and in contrast to $MoScO_3$ we see a more pronounced half metallic behavior. The minority band shows an indirect R−Γ gap of 3.82 eV and the majority spin band is strongly metallic with valence bands deep in the conduction band. Such a feature has potential application in spintronics. Table 2 presents a summary of the band structure results. For the sake of comparison the values for $CrScO_3$ is also shown from reference [16].

Table 2 The mbj electronic band gaps in the minority and majority spin channels for the XScO3 pervoskites

Pervoskite $XScO_3$	**Band-gap [eV]**			
	minority		majority	
$MoScO_3$	R− Γ Γ− Γ	3.61 3.64	Slightly metallic	No gap
$WScO_3$	R−Γ	3.82	Metallic	No gap
$CrScO_3$	Metallic	No gap	Γ− Γ	5.496

Preprints (www.preprints.org) | NOT PEER-REVIEWED | Posted: 23 November 2020 doi:10.20944/preprints202011.0573.v1

3.2 Magnetic properties

Although the TM are paramagnetc and individually do not show any magnetism, the Mo/$WScO_3$ pervoskites are magnetic. This is due the local environment and the complex interactions of the TM d orbitals with the Sc and O_2 atoms. Sc does not seem to play any major role in the magnetism as indicated by the spin polarized total density of states (TDOS) plots Fig. 3 and 4.

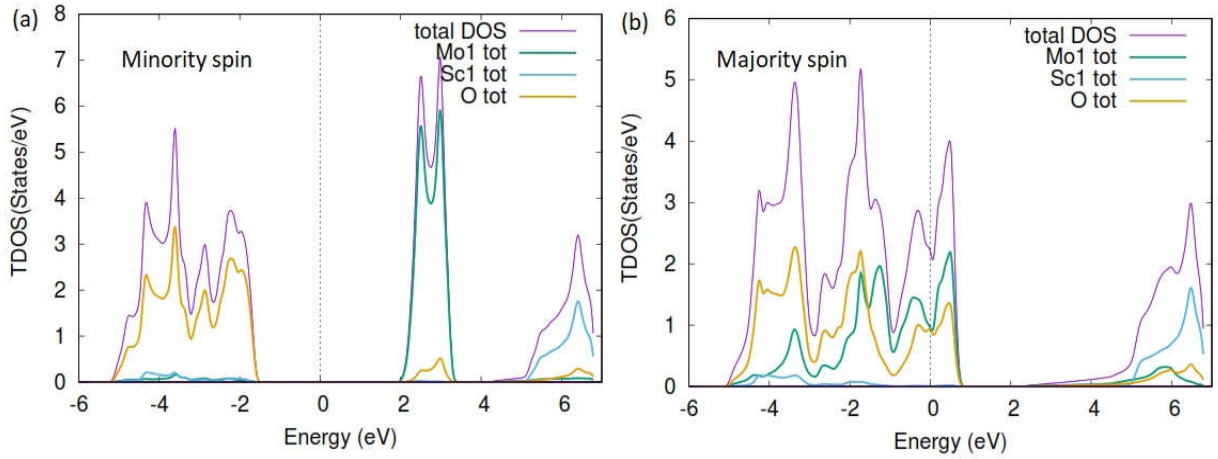

Fig. 4 The $MoScO_3$ electronic total density of states TDOS for the compound and the atom constituents in (a) minority and (b) majority spin channels

The TDOS of the minority spin of the compound shows clearly the forbidden energy gap, with the Mo DOS dominating the conduction band and oxygen states on the valence side of the TDOS. Meanwhile for the majority spin the TDOS of the compound and Mo and O_2 DOS have peaks around E-Fermi, clearly indicating a metallic behavior for $MoScO_3$ majority spin.

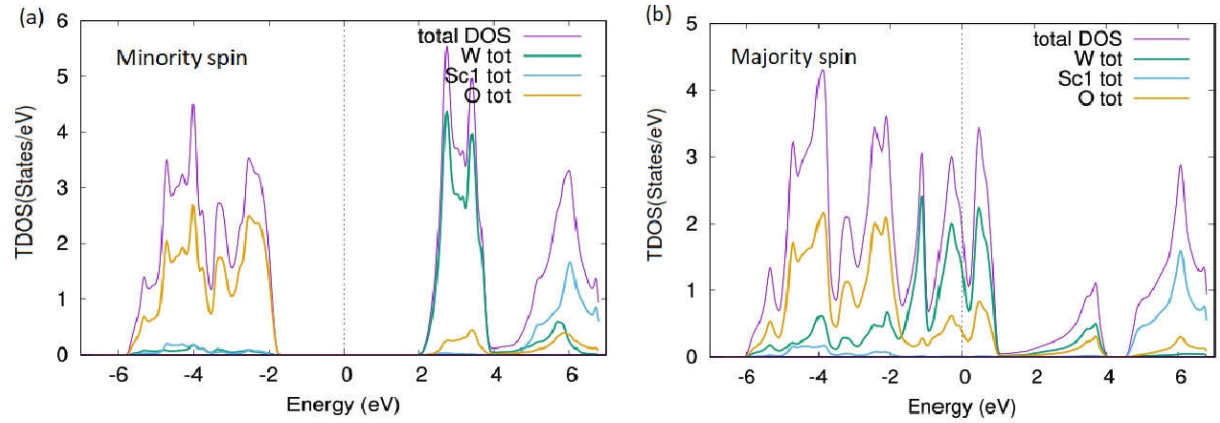

Fig. 5 The $WScO_3$ electronic total density of states TDOS for the compound and the atom constituents in (a) minority and (b) majority spin channels

The TDOS for WScO3 in Fig.5 shows a similar trend as in MoScO3, with minority spin showing the band gap and semiconducting nature, while, the majority TDOS has prominent peaks at E-Fermi belonging to the full compound, Mo and O_2 indicating the metallic behavior and showing

Preprints (www.preprints.org) | NOT PEER-REVIEWED | Posted: 23 November 2020 doi:10.20944/preprints202011.0573.v1

consistency with the band structure plots Figs. 2 and 3. In addition, we notice, that the TDOS for both the perovskite compounds in Figs. 4 and 5 shows a marked difference in the spin up and spin down density and this clearly gives rise to the magnetism with a magnetic moment of $2.99\mu_B$ in the two perovskites as shown in Table 3.

Table 3 lists the total magnetic moments: atom wise, interstitial and of the perovskite compounds. We notice from the table that the perovskites have very similar total moments. This is as expected since Mo and W belong to the same group VI elements and are isoelectric. The magnetic moment of the compounds arises mainly from the TM with unfilled d bands. For the sake of comparison the corresponding values for $CrScO_3$ has been included from reference [16].

Table 3 The total and atom projected magnetic moments of the $XScO_3$ perovskites in units of μ_B

Compound	X (Mo, W, Cr)	Sc	O	Intertitial	Total Moment
$MoScO_3$	2.957	0.006	-0.114	0.375	2.997
$WScO_3$	2.996	0.012	-0.144	0.417	2.994
$CrScO_3$	3.536	0.004	−0.215	0.101	2.999

3.3 Optical properties

Knowledge of the optical properties of a compound is crucial and fundamental for many applications and applied research. It is highly important to have a very dense grid and an accurate exchange correlation in the FP-LAPW to calculate the complex dielectric function that takes into account the self-energy and local field corrections. The TB-mBJ proves to be an excellent choice with a 30×30×30 grid for our optical properties calculations to obtain a high degree of accuracy of results. In this section we present the results for the dielectric function, optical conductivity and the important optical constants namely, the refractive index, the reflectivity, the extinction and absorption coefficients.

The complex dielectric function ($\varepsilon = \varepsilon_1 + i\varepsilon_2$) is a function of the amount of light absorbed by the material. The imaginary part of dielectric function, $\varepsilon_2(\omega)$, which represents absorption behavior, can be calculated from the electronic band structure of solids [23]. The real part of dielectric function, $\varepsilon_1(\omega)$, can be calculated according to Kramers-Kroing relation [24, 25] which represents the electronic polarization under incident light. Fig. 6 shows the real and imaginary plots for the dielectric function for the Mo/$WScO_3$ perovskites in the photon energy range of 0-14eV. We see from the plots that the active spectral region is within 2eV, beyond which the graphs are flat. The static dielectric constants are those at $\omega=0$, and we notice that the ε_1 value of $MoScO_3$ is more than double that of $WScO_3$ indicating a very much higher dielectric constant. The negative values for $\varepsilon_1(\omega)$ indicate a metal like behavior in these very low photon energies with complete reflection of light. Moreover, in Fig.6(b) the $\varepsilon_2(\omega)$ peaks are also more than twice that of $WScO_3$, implying much higher absorption capabilities. The peaks occur at low photon energy around 1 eV and indicate transitions of valence oxygen ‘2p’ electrons to low lying conduction 4/5d bands.

Preprints (www.preprints.org) | NOT PEER-REVIEWED | Posted: 23 November 2020 doi:10.20944/preprints202011.0573.v1

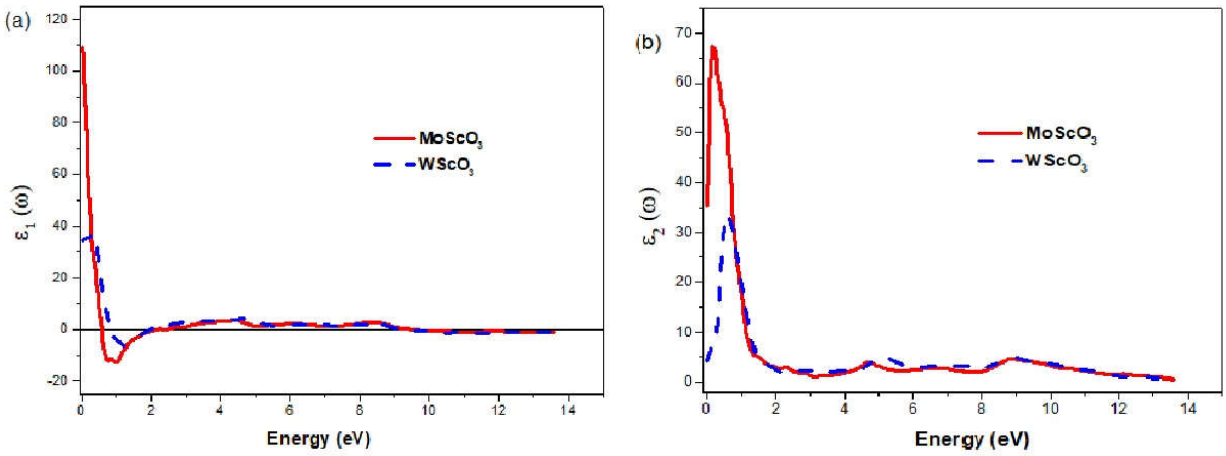

Fig. 6 The Mo/WScO$_3$ dielectric functions (a) the real part $\varepsilon_1(\omega)$ and (b) the imaginary part $\varepsilon_2(\omega)$

The complex index of refraction of the medium N is defined as

$$N = \sqrt{\varepsilon} = n + ik \qquad (1)$$

Where, n is the usual refractive index and k is the extinction coefficient. Using the values of ε_1 and ε_2 we can obtain the refractive index n, reflectivity, and the extinction and absorption coefficients from the equations (2) (3), (4) and (5)

$$R(\omega) = \frac{n+ik-1}{n+ik+1} \qquad (2)$$

$$n(\omega) = \left[\frac{\sqrt{{\varepsilon_1}^2(\omega) + {\varepsilon_2}^2}(\omega) + \varepsilon_1(\omega)}{2}\right]^{\frac{1}{2}} \qquad (3)$$

$$k(\omega) = \left[\frac{\sqrt{{\varepsilon_1}^2(\omega) + {\varepsilon_2}^2}(\omega) - \varepsilon_1(\omega)}{2}\right]^{\frac{1}{2}} \qquad (4)$$

$$\alpha(\omega) = \sqrt{2}\left[\sqrt{{\varepsilon_1}^2(\omega) + {\varepsilon_2}^2}(\omega) - \varepsilon_1(\omega)\right]^{\frac{1}{2}} \qquad (5)$$

The refractive index and reflectivity plots are shown in Fig. 7(a) and (b) respectively in the photon energy range 0-14eV, which captures all the necessary features. Refractive index is a function of incident frequency and the graphs display maximum peak values around ω =0, with a decrease in values as we go towards higher frequencies. Both MoScO$_3$ and WScO$_3$ have large refractive index values of 10.6 and 5.7 respectively as a result of the high electron densities in these materials [5]. The refractive index shows an almost constant and optically isotropic behavior at high energies > orange. The reflectivity is a maximum in the visible energy range, and the materials could be used be used as reflective coatings in this range. Beyond this we

Preprints (www.preprints.org) | NOT PEER-REVIEWED | Posted: 23 November 2020 doi:10.20944/preprints202011.0573.v1

observe an almost constant region with very small reflectance values in 3-8 and 2-8eV for $MoScO_3$ and $WScO_3$ respectively. This region of the spectra therefore provides good ultraviolet (UV) and higher energy absorption. It is well known that the materials with band gaps larger than 3.1 eV as in the present case, work well for applications in the UV region of the spectrum [26]. After 8eV we see steady increases to reach ~0.6 for both compounds.

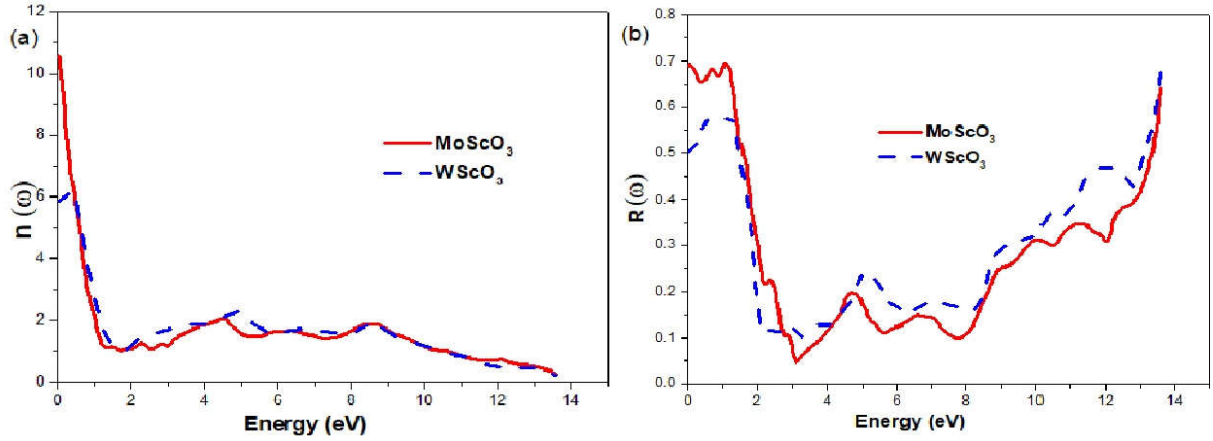

Fig. 7 The Mo/$WScO_3$ optical constants (a) refractive index n(ω) and (b) the reflectivity R(ω) as a function of the photon energies

In Table 4 we list the energies of the zeros of $\varepsilon_1(\omega)$ and static values of the refractive index, the reflectivity and absorption coefficients.

Table 4 The zero y-values of $\boldsymbol{\varepsilon_1(\omega)}$ and the static optical constants at ω=zero; dielectric constant $\varepsilon_1(0)$, static refractive index n(0), static reflectivity R(0) and static absorption coefficient I(0) XScO3 perovskite compounds.

Compound	**Zeros of $\varepsilon_1(\omega)$ [eV]**	**$\varepsilon_1(0)$**	**n(0)**	R(0)	I(0)
$MoScO_3$	2.163eV ; 2.435	109.052	10.576	0.691	0.231
$WScO_3$	0.829 ; 1.946	34.329	5.869	0.504	0.351

Preprints (www.preprints.org) | NOT PEER-REVIEWED | Posted: 23 November 2020 doi:10.20944/preprints202011.0573.v1

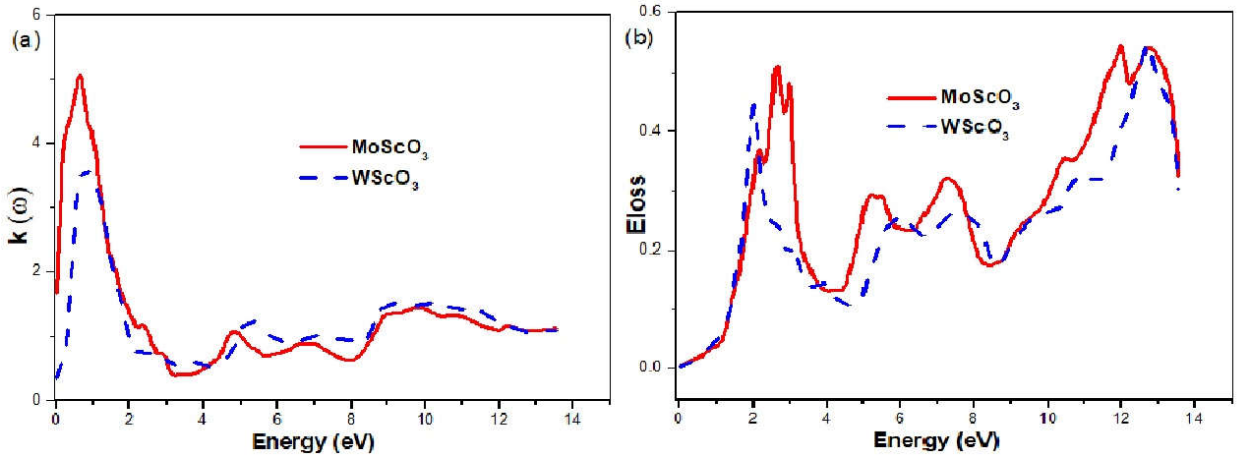

The optical conductivities and absorption coefficients are shown in Fig 8. From the graphs we notice that both the pervoskites have good optical conductivities in the visible range and also high absorption coefficients making them excellent for optoelectronic applications.

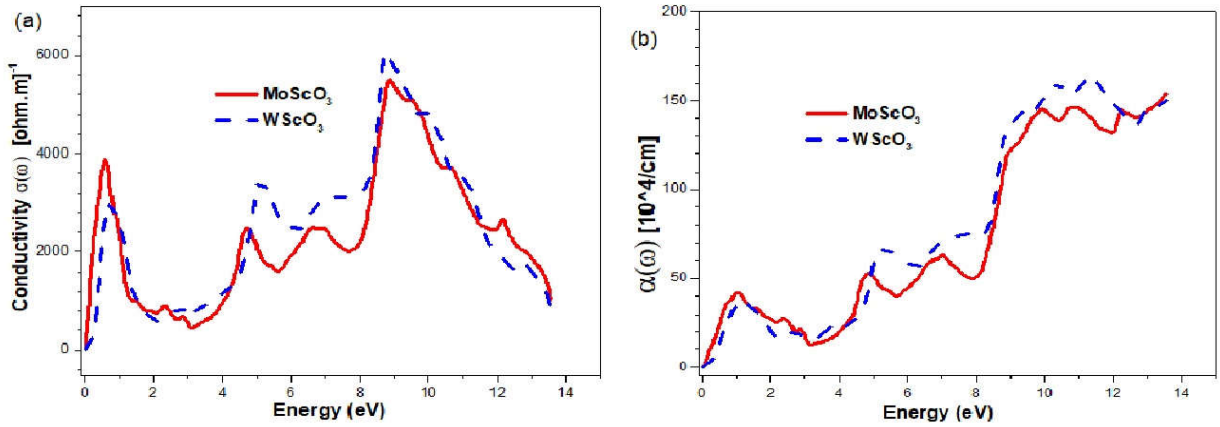

Fig. 9 The Mo/$WScO_3$ (a) optical conductivity σ (ω) and (b) absorption coefficient I(ω) as a function of the photon energies

4. Conclusions

In conclusion, this is the first investigation of the pervoskites Mo/$WScO_3$ using DFT, full potential linearized augmented plane wave method with mBJ approximation to obtain accurate electronic, band structures, magnetic and optical properties. The results indicate that the compounds are half metals with semiconducting in the minority and metallic behaviour in the majority spin channels. Moreover the considerable band gap and sizeable magnetic moment makes these materials very suitable for spintronic applications.

In addition the optical spectral properties in the energy range of 0-14eVfor the dielectric function and optical constants gives a reliable and through understanding of potential application of these

materials in opto-electronics, as the first principles DFT-mBJ is a powerful tool and predicts the important electronic and band-structure related properties with high accuracy.

References

1. Mannhart, J.; Schlom, D. G. (25 March 2010). "Oxide Interfaces--An Opportunity for Electronics". *Science*. **327** (5973):1607-1611. doi:10.1126/science.1181862
2. Kulkarni, A; FT Ciacchi; S Giddey; C Munnings; et al. (2012). "Mixed ionic electronic conducting perovskite anode for direct carbon fuel cells". *International Journal of Hydrogen Energy*. **37**(24): 19092–19102
3. Hodes, G. (2013). "Perovskite-Based Solar Cells". *Science*. **342** (6156): 317–318.
4. Johnsson, Mats; Lemmens, Peter (2007). "Crystallography and Chemistry of Perovskites". *Handbook of Magnetism and Advanced Magnetic Materials*. arXiv:cond-mat/0506606. doi:10.1002/9780470022184.
5. K.E. Babu, A. Veeraiah, D.T. Swamy, V. Veeraiah, First-principles study of electronic structure and optical properties of cubic perovskite $CsCaF_3$, Chin. Phys. Lett. 29 (11) (2012) 117102.
6. Hayatullah, G. Murtaza, R. Khenata, S. Muhammad, A.H. Reshak, Kin Mun Wong, S. Bin Omran, Z.A. Alahmed, Structural, chemical bonding, electronic and magnetic properties of KMF3 (M = Mn, Fe, Co, Ni) compounds, Comput. Mater. Sci. 85 (2014) 402–408.
7. P D Sesion Jr, J M Henriques, CCABarboza, E L Albuquerque, V NFreire and E W S Caetano, Structural, electronic and optical properties of ilmenite and perovskite CdSnO3 from DFT calculations (2010) J. Phys.: Condens. Matter 22 435801
8. Murat Aycibin and Naciye ECE, First-principles calculation of the electronic and optical properties of BiRhO3 compound AIMS Materials Science (2017) 4(4) 894-904.
9. A.A Ramanathan, J.M Khalifeh, Substrate matters: Magnetic tuning of the Fe monolayer, Journal of Magnetism and Magnetic Materials (2017) 426, 450-453
10. H. Cai, Y. Guo, H. Gao, W. Guo, Tribo-piezoelectricity in Janus transition metal dichalcogenide bilayers: a first-principles study, Nano Energy 56 (2019) 33–39.

11. J. T. Wang and C. Zhang, Magnetic Field Effect on Dielectric Properties of Pb(Fe0.5Nb0.5)O3 (PFN), Ferroelectrics **301**, 211 (2004).

12. A.A Ramanathan, J.M Khalifeh, BA Hamad, Structure and magnetism of the V/Ta(0 01) surface: A DFT calculation, Journal of magnetism and magnetic materials (2009) 321 (22), 3804-3807

13. A.A Ramanathan, Khalifeh, J.M., Hamad, B. A DFT study of substrate effect on the magnetism of V(001) surface, Surf. Sci., (2011) 605, 1074-1076

14. Kimura, T., Goto, T., Shintani, H. *et al.* Magnetic control of ferroelectric polarization. *Nature* **426,** 55–58 (2003). https://doi.org/10.1038/nature02018

15. Maksym V. Kovalenko, Loredana Protesescu and Maryna I. Bodnarchuk Properties and potential optoelectronic applications of lead halide perovskite nanocrystals, Science (2017) 358 (6364), 745-750

16. N. Mahmoud, B. Almalaji, A. Mousa, J. Khalifeh Effect of the"3-d" band filling on the structural, electronic, magnetic and optical properties of $TMScO_3$ perovskite, Chin J Phys, (2020) 65, 500-512

17. P. Blaha, K.Schwarz, F. Tran, R. Laskowski, G.K.H. Madsen and L.D. Marks, J. Chem. Phys. (2020) 152, 074101

18. W. Kohn, L.J. Sham, Self-Consistent equations including exchange and correlation effects, Phys. Rev. 140A (1965) 1133.

19. J. P. Perdew, K. Burke, and M. Ernzerhof, Generalized Gradient Approximation Made Simple, Phys. Rev. Lett. (1996) 77, 3865

20. F. Tran, P. Blaha, Accurate band gaps of semiconductors and insulators with a semilocal exchange-correlation potential, Phys. Rev. Lett. 102 (2009) 226401.

21. Peter E. Blo¨ chl, O. Jepsen, O.K. Andersen, Phys. Rev. B 49 (1994) 16223.

22. F.D. Murnaghan, The compressibility of media under extreme pressures, Proc. Natl. Acad. Sci. 30 (1944) 244–247.

23. M. Dressel, G. Gruner, Electrodynamics of Solids: Optical Properties of Electrons in Matter, Cambridge University Press, UK, 2002.

 doi:10.20944/preprints202011.0573.v1

24. Kramers H A 1927 Atti del Congresso Internazionale dei Fisici vol 2 (Bologna: Zanichelli) p 545

25. Kronig R de L 1926 J. Opt. Soc. Am. 12 547

26. M. Maqbool, B. Amin, I. Ahmad, Bandgap investigations and the effect of the In and Al concentration on the optical properties of InxAl1−xN. J. Opt. Soc. Am. B (2009) 26, 2180

27.